Ramirez Hoyos, P.; Gómez Lozano, V.; Ali, M.; Ensinger, W.; Mafé, S. (2013). Net currents obtained from zero-average potentials in single amphoteric nanopores. Electrochemistry Communications. 31:137-140. doi:10.1016/j.elecom.2013.03.026.

Net currents obtained from zero-average potentials in single amphoteric nanopores

Patricio Ramirez [a,*], Vicente Gomez [a], Mubarak Ali [b,c], Wolfgang Ensinger [b], Salvador Mafe [d,*]

[a] *Dept. de Física Aplicada. Univ. Politècnica de València. E-46022 Valencia, Spain*

[b] *Department of Material- and Geo-Sciences, Materials Analysis, Technische Universität Darmstadt, Petersenstr.23, D-64287 Darmstadt, Germany*

[c] *Materials Research Department, GSI Helmholtzzentrum für Schwerionenforschung, Planckstrasse 1, D-64291, Darmstadt, Germany*

[d] *Dept. de Física de la Terra i Termodinàmica, Universitat de València, E-46100 Burjassot, Spain*

ABSTRACT

We have studied experimentally and theoretically the rectifying properties of a single asymmetric nanopore functionalized with amphoteric lysine groups and characterized the net current obtained with zero-average time dependent potentials. The pH-controlled rectification phenomena may be relevant to bio-electrochemistry, pH sensing and regulation, and energy conversion.

Keywords:

Nanofluidic ratchet, amphoteric pore, rectification, pH sensing and regulation, energy conversion

---

* Corresponding authors. E-mail addresses: patraho@fis.upv.es (P. Ramirez) and smafe@uv.es (S. Mafe).

1. Introduction

When Brownian particles are subject to driving forces showing time correlations, net currents can be obtained from zero-average forces in ratchet systems [1-5]. Ratchet-based procedures are useful in gel electrophoresis [6] and electronic switching in logic circuits [7]. The ion channels of biological membranes and the nanofluidic pores constitute soft matter versions of solid state diodes that are able to drive an electric current under zero-average time dependent potentials [8-12]. The nanopores exhibiting rectification characteristics [13-15] are useful for separation, information processing, and energy harvesting applications [8, 16-18].

Conical nanopores track-etched in polymer films can be patterned with asymmetric regions of positive and negative charges that are tuned electrochemically, allowing the nanofluidic diodes to act as liquid-state transistors [13-15, 17, 19-21]. While a clear understanding of the pore response to external stimuli (voltage, temperature, *pH* and UV light) has already been achieved [14, 20-26], practical applications are still emerging. We demonstrate here that a pH-controlled net current can be obtained with a single asymmetric nanopore functionalized with amphoteric lysine groups in the case of zero-average time-dependent potentials, suggesting some practical applications of the concept.

2. Experimental section

Single conical nanopores with openings ranging from a few (tip) to hundreds (base) of nanometers were fabricated in polyethylene terephthalate membranes by track-etching techniques [23]. The pore incorporated the amino acid L-lysine as an amphoteric chain with two ionizable residues, one carboxylic group and one amino group.

3. Results and discussion

Fig. 1A shows the pore geometry [23], the time-dependent potential $V(t)$, and the current I. We use the conical model instead of the more elaborated funnel-like model [19] for the sake of simplicity. Fig. 1B shows $I(t)$ and $V(t)$ at pH = 11 (negatively charged pore) and pH = 2 (positively charged pore). The rectification can be influenced by the potential scan rate [27, 28], achieving a maximum value at low rates [27, 28]. While the (nanoscale) radial diffusion is relatively fast, diffusion over the (microscale) axial distances takes times higher than $\tau = L^2/D_k = 0.1$ s, where $L = 12$ μm is the pore length and $D_k = 10^{-9}$ m^2/s is the ionic diffusion coefficient. We will not be concerned with the different pore response regimes [27, 28] because we consider only scan rates low enough for the pore to be slave of the input signal (the frequency of the input signal should then be much lower than 10 Hz, which is the case of Fig. 1B).

Fig. 1C shows the quasi-steady state experimental current-voltage (I-V) curves obtained from experiments similar to those of Fig. 1B. All data correspond to 0.1 M KCl aqueous solutions. The curves reflect a progressive change in the pore charge between low pH (the amino group -NH_3^+ is positively charged while the carboxylic group –COOH is neutral) and high pH (–NH_2 is neutral while –COO^- is negatively charged). The rectification properties are reversed around the lysine isoelectric point pI = 5.6 (zero net charge) [23].

Fig. 1D shows the zero-average external potentials used here to obtain the net currents $<I>$ averaged over a signal period. At the low scan rates of Fig. 1B, $I(t)$ should follow closely the input signals $V_i(t)$ (see also Fig. 2 of Ref. [29] for other nanopores and Fig. 3 of Ref. [10] for the case of ion channels). Therefore, $<I>$ can be estimated from the experimental currents of Fig. 1C invoking the adiabatic limit [3-5]:

$$< I >= \frac{1}{2}\left[(1-\gamma) I\left(V_0 \frac{1+\gamma}{1-\gamma} \right) + (1+\gamma) I\left(-V_0 \right) \right] \quad (i = 1) \tag{1}$$

$$< I >= \frac{1}{2}\left[I\left(V_0\right) + I\left(-V_0\right)\right] \quad (i = 2) \tag{2}$$

$$< I >= \frac{1}{2}\left[(1+\gamma) I\left(V_0\right) + (1-\gamma) I\left(-\frac{1+\gamma}{1-\gamma} V_0 \right)\right] \quad (i = 3) \tag{3}$$

where γ = 1/2 for the $V_i(t)$ of Fig. 1D. All the average currents <*I*> of Figs. 1-3 have been calculated using Eqs. (1)-(3).

Fig. 1E shows the <*I*> *vs.* V_0 curves obtained introducing in Eqs. (1)-(3) the experimental data of Fig. 1C for pH = 2 and 11. We used the potential amplitude V_0 because of its direct experimental access (note also that this parameter of the driving force is used in most theoretical models). The results can be compared with those reported by Siwy *et. al* for ion pumping in negative pores [11, 12, 29]. While the input driving forces have zero-average values over a time period (Fig. 1D), the average outputs <*I*> are non-zero because of the nanopore rectification (Fig. 1C).

Fig. 1F shows the corresponding theoretical curves where <*I*> is also estimated from Eqs. (1)-(3), but now with the quasi-steady state *I*-*V* curves [23] obtained by solving the Nernst-Planck flux equations [13, 30, 31]

$$\vec{J}_k = -D_k \left(\vec{\nabla} c_k + z_k c_k \vec{\nabla} \phi \right) \tag{4}$$

and the Poisson equation

$$\nabla^2 \phi = -\frac{F^2}{\varepsilon RT} \left(\sum_k z_k c_k + X_F \right) \tag{5}$$

where $\vec{J}_k$, c_k, and z_k are the flux, local concentration, and charge number of ion *k*, respectively; ε is the electric permittivity of the solution and constants *F*, *R*, and *T* have their usual meaning [23], ϕ is the electric potential (normalized to *RT*/*F*), and X_F is the volume

concentration of the pore fixed charge [13]. Note that X_F should be obtained by solving the pH-controlled dissociation equilibrium for the $–NH_3^+$ and –COOH groups [23, 32]. The electric potential and concentrations at $x = 0$ and $x = L$ (Fig. 1A) are calculated in terms of those in the external solutions using the Donnan equilibrium at the respective pore-solution interfaces (the access resistances can be neglected because the pore is long and narrow) [13, 23]. The resulting equation system is integrated using iterative schemes to obtain the ionic fluxes, and then the electric current *I*, at voltage *V*. This procedure gives theoretical *I*-*V* curves similar to the experimental curves shown in Fig. 1C [23]. The contribution of the hydrogen ion to these curves is ignored because the KCl concentration is 0.1 M while pH > 2 for most of the cases.

Fig. 1F shows the pore parameters used in the calculations. The radius of the cone base (165 nm) is measured directly by using FESEM techniques in multi-pore polymer samples etched simultaneously with the single pore sample [23]. The tip radius (8 nm) is obtained by fitting the linear *I*-*V* curve measured for the neutral pore at the lysine isoelectric point to the model predictions. Once the pore radii are known, the surface density of active groups *N* (0.6 lysine groups per square nanometer) is obtained by fitting the non-linear *I*-*V* curves measured at pH = 2 and pH = 11 (note that X_F can be obtained from *N* at each pH [32]).

Figs. 2A-C show the $\langle I \rangle$ *vs.* V_0 curves obtained substituting the experimental currents of Fig. 1C that correspond to the potential amplitudes of Fig. 1D directly into Eqs. (1)-(3). Figs. 2D-F show the theoretical results obtained following the numerical procedure used in Fig. 1F. Finally, Figs. 3A (experiment) and 3B (theory) show $\langle I \rangle$ *vs.* pH at fixed V_0. As expected, $\langle I \rangle$ increases (in absolute value) when the pH values deviate progressively from the pore isoelectric point. The symmetrical potential $V_2(t)$ of Fig. 1D gives low net currents while

the asymmetrical potentials $V_1(t)$ and $V_3(t)$ give high currents when combined with the appropriate asymmetry and sign of the pore charge distribution. This fact is a consequence of the rectification shown by the *I-V* curves (Fig. 1C). The comparison of the theoretical calculations with the experimental data shows that the model accounts for the results obtained under a wide range of *pH* conditions

Incidentally, the electrostatic gating (gate potential $V_G(t)$) of a pore could also be implemented [20, 22, 33] instead of the chemical gating (pH) used here, thus removing the need of external pH control. Also, the effects of signal mixing (potentials $V_i(t)$ and $V_G(t)$) on $\langle I \rangle$ may be exploited to implement a logic operations scheme [22, 34].

4. Conclusions

We have studied experimentally and theoretically the rectifying properties of a single asymmetric nanopore functionalized with amphoteric groups (L-lysine chains) and the pH-controlled net current obtained with zero-average potentials. The results are reminiscent of those found in ratchet systems [9] and constitute a significant extension with respect to previous studies by Siwy *et al.* [11, 12, 29]. The observed effects could be enhanced further by exploiting pH gradients [35]. Rectification and signal averaging of weak electric fields (in particular, the problem of dc currents generated by external ac signals [36, 37]) are important for biological cells and then this study may also have some bio-electrochemical relevance.

Potential applications concern pH sensing and regulation in chemical processors [17, 21, 38] and pulsatile ionic transport triggered by particular pH conditions deviating from the prescribed acidic or basic target regions [39]. Other areas of interest are electrochemical charge storage [7, 16, 18] and logic switching [7, 17] in liquid state ionics because a multi-pore asymmetric membrane could work as a voltage-controlled current source when

connected to an external load capacitor, allowing thus the conversion between the net current caused by the periodic potential and the output voltage.

Acknowledgements

P. R., V. G., and S. M. acknowledge the Ministry of Economy and Competitiveness (project MAT2012-32084) and the Generalitat Valenciana (project PROMETEO/GV/0069). M. A. and W. E. acknowledge the Beilstein-Institut, Frankfurt/Main, Germany, within the research collaboration NanoBiC. The authors thank Dr. Christina Trautmann from GSI for support with the heavy ion irradiation experiments.

References

[1] R. D. Astumian, P. Hänggi, Phys. Today 55 (2002) 33-39.

[2] A. Ajdari, J. Prost, C. R. Acad. Sci. Paris 315 (1992) 1635-1639.

[3] M. O. Magnasco, Phys. Rev. Lett. 71 (1993) 1477-1481.

[4] D. R. Chialvo, M. M. Millonas, Phys. Lett. A 209 (1995) 26-30.

[5] B. Ai, L. Wang, L. Liu, Phys. Rev. E 72 (2005) 031101.

[6] G. A. Griess, E. Rogers P. Serwer, Electrophoresis 22 (2001) 981–989.

[7] M. Kabir, D. Unluer, L. Li, A. W. Ghosh, M. R. Stan, *Electronic Ratchet: A Non-Equilibrium, Low Power Switch*, in *11th IEEE International Conference on Nanotechnology*, Portland, Oregon, USA (2011) 15-18.

[8] J. C. T. Eijkel, A. van den Berg, Microfluid Nanofluid 1 (2005) 249–267.

[9] P. Hänggi, F. Marchesoni, Rev. Mod. Phys. 81 (2009) 387-442.

[10] C. Verdiá-Báguena, M. Queralt-Martín, V. M. Aguilella, A. Alcaraz, J. Phys. Chem. C 116 (2012) 6537−6542.

[11] Z. Siwy, A. Fuliński, Phys. Rev. Lett. 89 (2002) 198103.

[12] Z. Siwy, A. Fuliński, Am. J. Phys. 72 (2004) 567-574.

[13] J. Cervera, B. Schiedt, R. Neumann, S. Mafe, P. Ramirez, J. Chem. Phys. 124 (2006) 104706.

[14] Z. S. Siwy, Adv. Funct. Mater. 16 (2006) 735–746.

[15] I. Vlassiouk, Z. Siwy, Nano Lett. 7 (2007) 552-556.

[16] J. Cervera, P. Ramirez, S. Mafe, P. Stroeve, Electrochim. Acta 56 (2011) 4504-4511.

[17] P. Ramirez, M. Ali, W. Ensinger, S. Mafe, Appl. Phys. Lett. 101 (2012) 133108.

[18] W. Guo, L. Cao, J. Xia, F.-Q. Nie, W. Ma, J. Xue, Y. Song, D. Zhu, Y. Wang, L. Jiang, Adv. Funct. Mater. 20 (2010) 1339-1344.

[19] P.Y. Apel, I. V. Blonskaya, O. L. Orelovitch, B. A. Sartowska, R. Spohr, Nanotechnology 23 (2012) 225503.

[20] W. Guan, R. Fan, M. A. Reed., Nat. Commun. 2 (2011) 506.

[21] L.-X. Zhang, X.-H. Cao, Y.-B. Zheng, Y.-Q. Li, Electrochem. Comm. 12 (2010) 1249–1252.

[22] S. Mafe, J. A. Manzanares, P. Ramirez, J. Phys. Chem. C 114 (2010) 21287-21290.

[23] M. Ali, P. Ramirez, S. Mafe, R. Neumann, W. Ensinger, ACS Nano 3 (2009) 603-608.

[24] M. Ali, S. Mafe, P. Ramirez, R. Neumann, W. Ensinger, Langmuir 25 (2009) 11993-11997.

[25] G. L. Wang, A. K. Bohaty, I. Zharov, H. S. White, J. Am. Chem. Soc. 128 (2006) 13553-13558.

[26] M. Ali, S. Nasir, P. Ramirez, I. Ahmed, Q. H. Nguyen, L. Fruk, S. Mafe, W. Ensinger, Adv. Funct. Mater. 22 (2012) 390-396.

[27] D. Momotenko, H. H. Girault, J. Am. Chem. Soc. 133 (2011) 14496–14499.

[28] J. P. Guerrette, B. Zhang, J. Am. Chem. Soc. 132 (2010) 17088–17091.

[29] E. Kalman, K. Healy, Z. S. Siwy, Europhys. Lett. 78 (2007) 28002.

[30] J. Cervera, P. Ramirez, J. A. Manzanares, S. Mafe, Microfluid. Nanofluid. 9 (2010) 41-53.

[31] K. Kontturi, L. Murtomäki, J. A. Manzanares, *Ionic Transport Processes* (Oxford University press, Oxford, 2008).

[32] S. Nasir, P. Ramirez, M. Ali, I. Ahmed, L. Fruk, S. Mafe, W. Ensinger, J. Chem. Phys. 138 (2013) 034709.

[33] N. Hu, Y. Ai, S. Qian, Sens. Actuators B 161 (2012) 1150– 1167.

[34] J. Cervera, S. Mafe, ChemPhysChem 11 (2010) 1654-1659.

[35] M. Ali, P. Ramirez, Q. H. Nguyen, S Nasir, J. Cervera, S. Mafe, W. Ensinger, ACS Nano 6 (2012) 3631-3640.

[36] R. D. Astumian, J. C. Weaver, R. K. Adair, Proc. Natl. Acad. Sci. 92 (1995) 3740-3743.

[37] J. A. Manzanares, J. Cervera, S. Mafe, Appl. Phys. Lett. 99 (2011) 153703.

[38] E. O. Gabrielsson, K. Tybrandt, M. Berggren, Lab Chip 12 (2012) 2507-2513.

[39] G. Jeon, S. Y. Yang, J. Byun, J. K. Kim, Nano Lett. 11 (2011) 1284-1288.

Figure captions

Fig. 1

(A) Scheme of the conical nanopore of radii a_L and a_R. (B) $I(t)$ and $V(t)$ *vs.* time t at pH = 11 and pH = 2. (C) Experimental *I-V* curves obtained at different pH values in 0.1 M KCl aqueous solutions. (D) Schemes of the zero-average input potentials $V_i(t)$ (i = 1, 2, 3) with characteristic amplitude V_0. (E) $\langle I \rangle$ *vs.* V_0 curves obtained over a time period of the potentials in Fig. 1D. The insets show the charge state of the amino acid groups at high and low pH. (F) Theoretical $\langle I \rangle$ *vs.* V_0 curves calculated with $pK_{a,1}$ = 3 and $pK_{a,2}$ = 9.0 [32], which are close to the tabulated values.

Fig. 2

(A)-(C) $\langle I \rangle$ *vs.* V_0 curves for the potentials of Fig. 1D at different pH values. (D)-(F) Theoretical $\langle I \rangle$ *vs.* V_0 curves.

Fig. 3

(A) $\langle I \rangle$ *vs.* pH curves at V_0 = 0.5 V. (B) Theoretical $\langle I \rangle$ *vs.* pH curves.

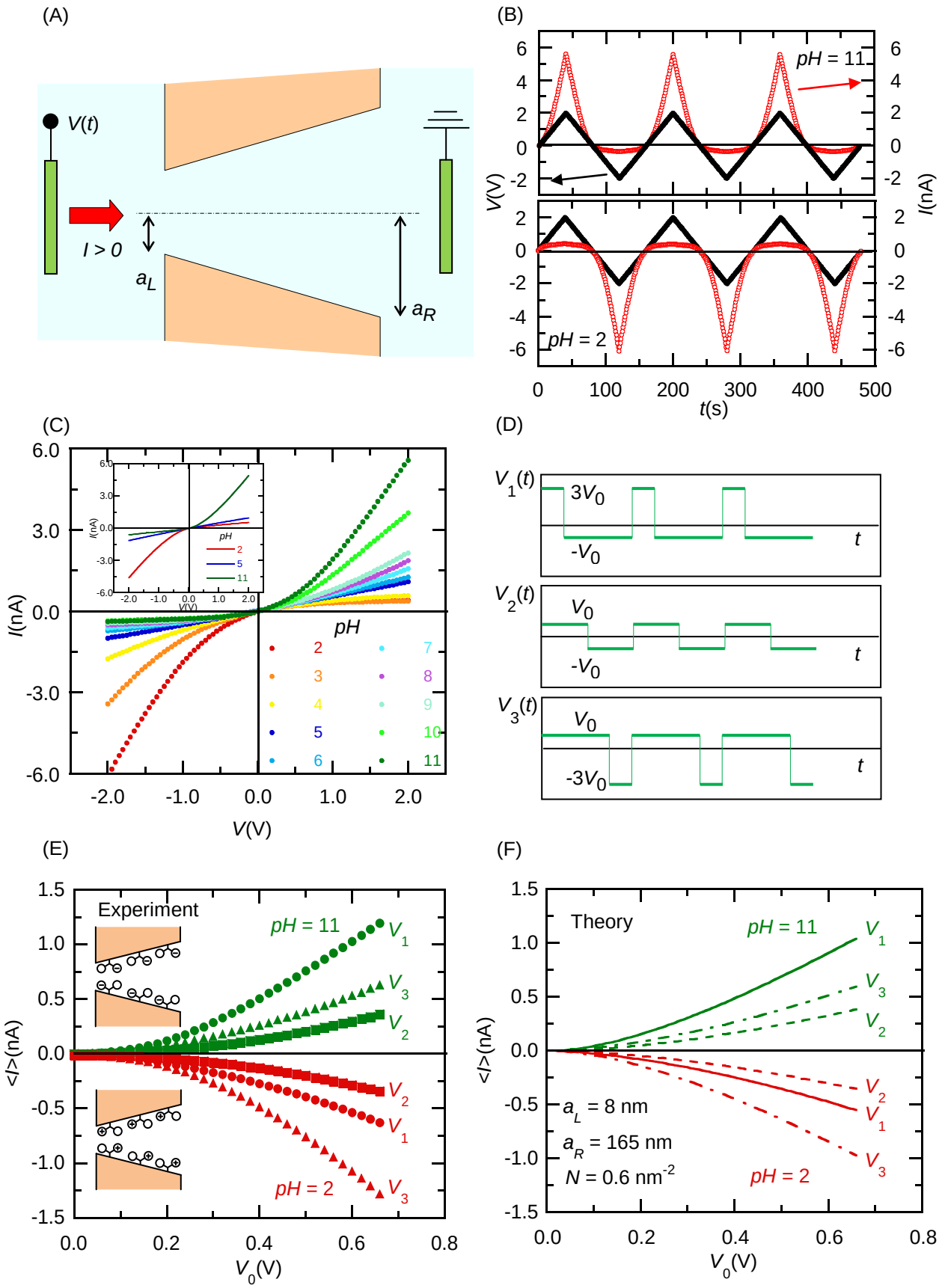
(A)
V(t)
I > 0
a_L
a_R
(B)
pH = 11
pH = 2
V(V)
I(nA)
t(s)
(C)
I(nA)
V(V)
pH
2
3
4
5
6
7
8
9
10
11
(D)
V_1(t)
3V_0
-V_0
t
V_2(t)
V_0
-V_0
t
V_3(t)
V_0
-3V_0
t
(E)
Experiment
pH = 11
pH = 2
V_1
V_2
V_3
<I>(nA)
V_0(V)
(F)
Theory
pH = 11
pH = 2
a_L = 8 nm
a_R = 165 nm
N = 0.6 nm^-2
V_1
V_2
V_3
<I>(nA)
V_0(V)

Figure 1

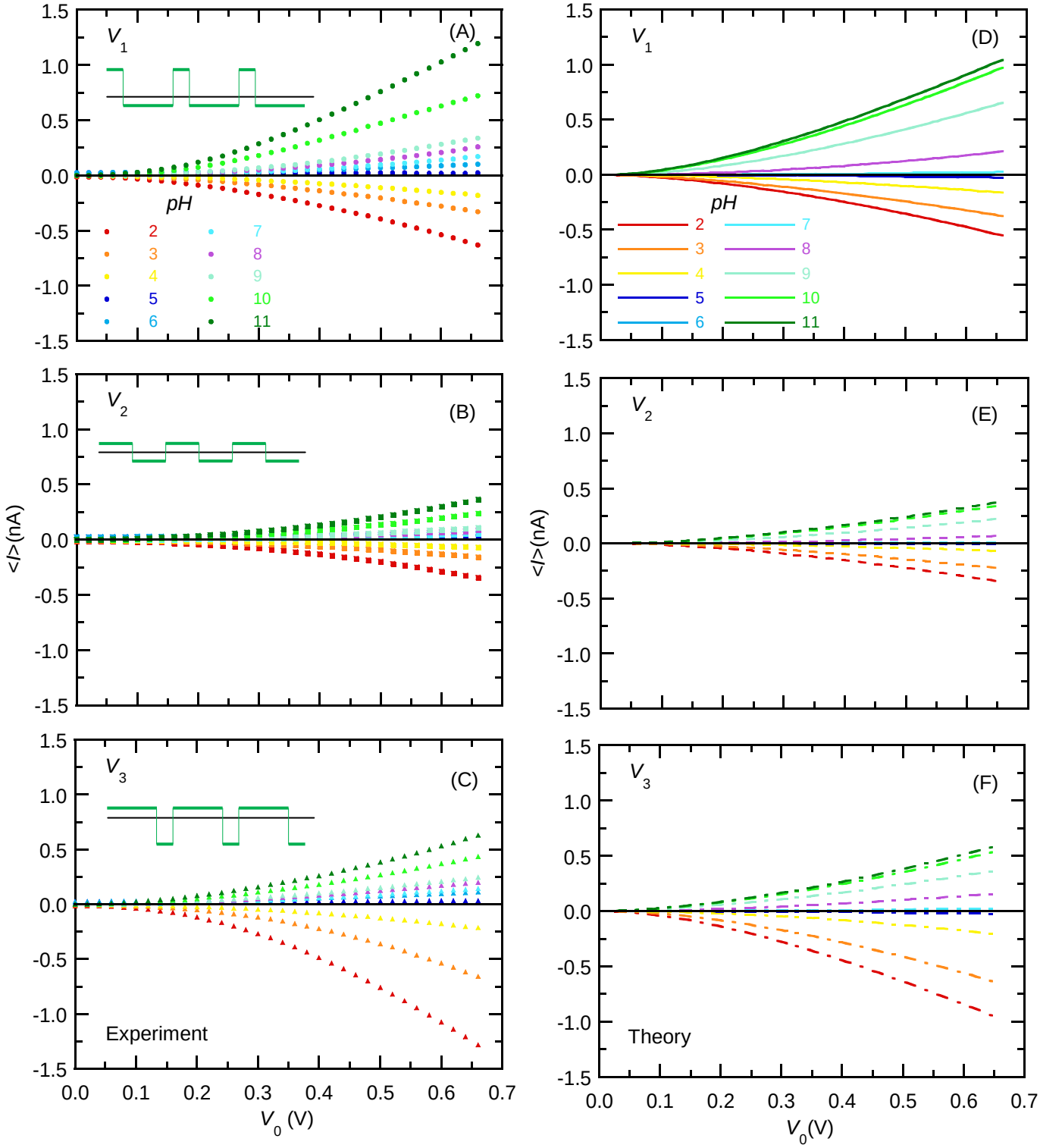

Figure 2

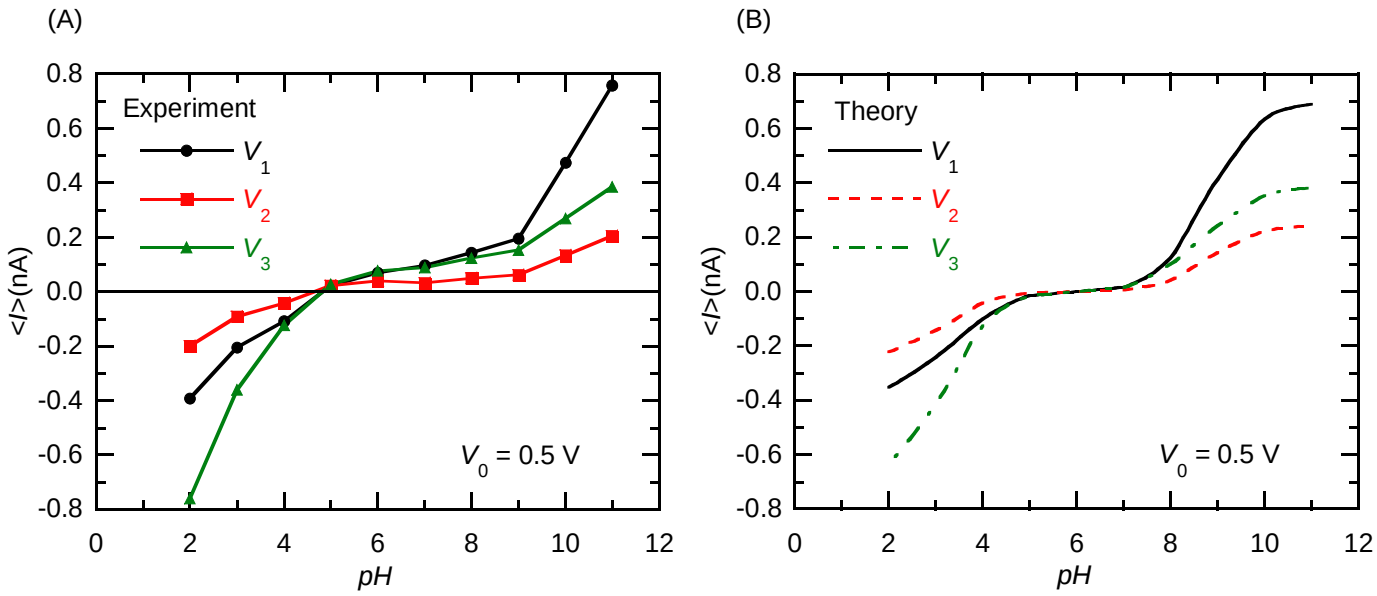
(A)
Experiment
V_1
V_2
V_3
V_0 = 0.5 V
<I>(nA)
pH
(B)
Theory
V_1
V_2
V_3
V_0 = 0.5 V
<I>(nA)
pH

Figure 3

Net Currents from Zero-average Potentials in Nanopores

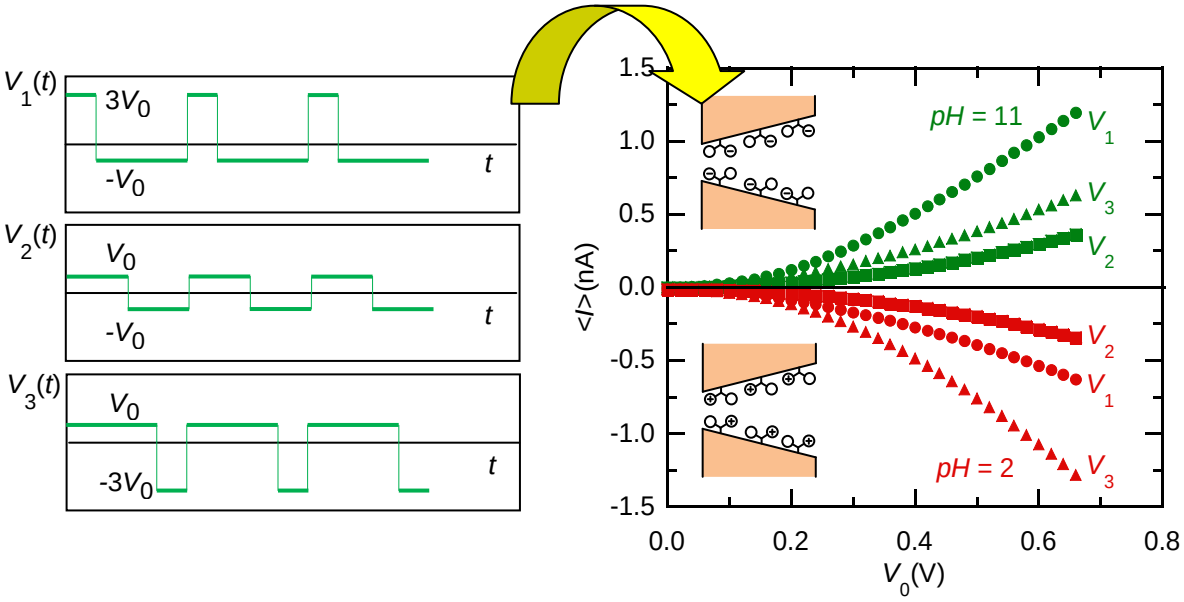

Graphical abstract